CENTER FOR ADVANCED SYSTEMS UNDERSTANDING

www.casus.science

Quantum linear and non-linear density response of electrons in warm dense matter

Zhandos Moldabekov

HELMHOLTZ ZENTRUM DRESDEN ROSSENDORF
TECHNISCHE UNIVERSITÄT DRESDEN
CBG Max Planck Institute of Molecular Cell Biology and Genetics
UFZ HELMHOLTZ Centre for Environmental Research
Uniwersytet Wrocławski
SPONSORED BY THE Federal Ministry of Education and Research
STAATSMINISTERIUM FÜR WISSENSCHAFT KULTUR UND TOURISMUS
Freistaat SACHSEN

Warm Dense Matter

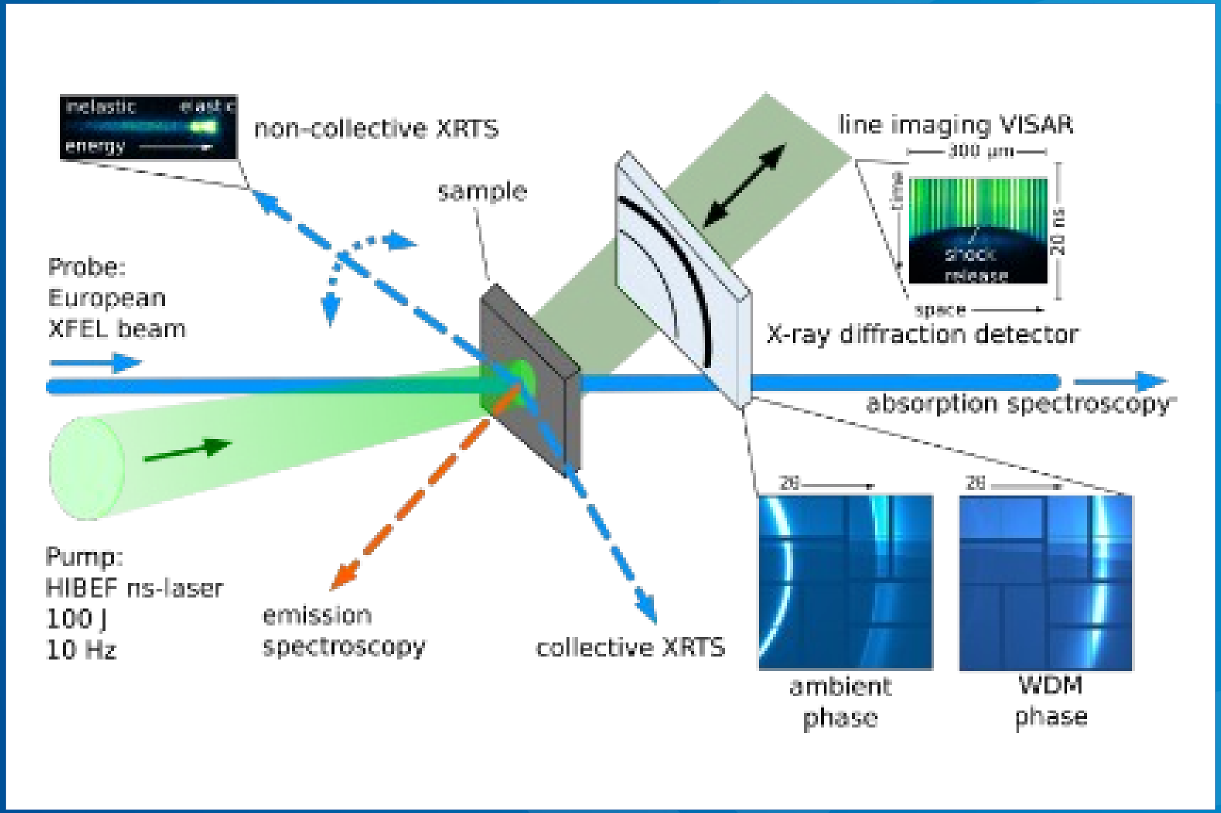

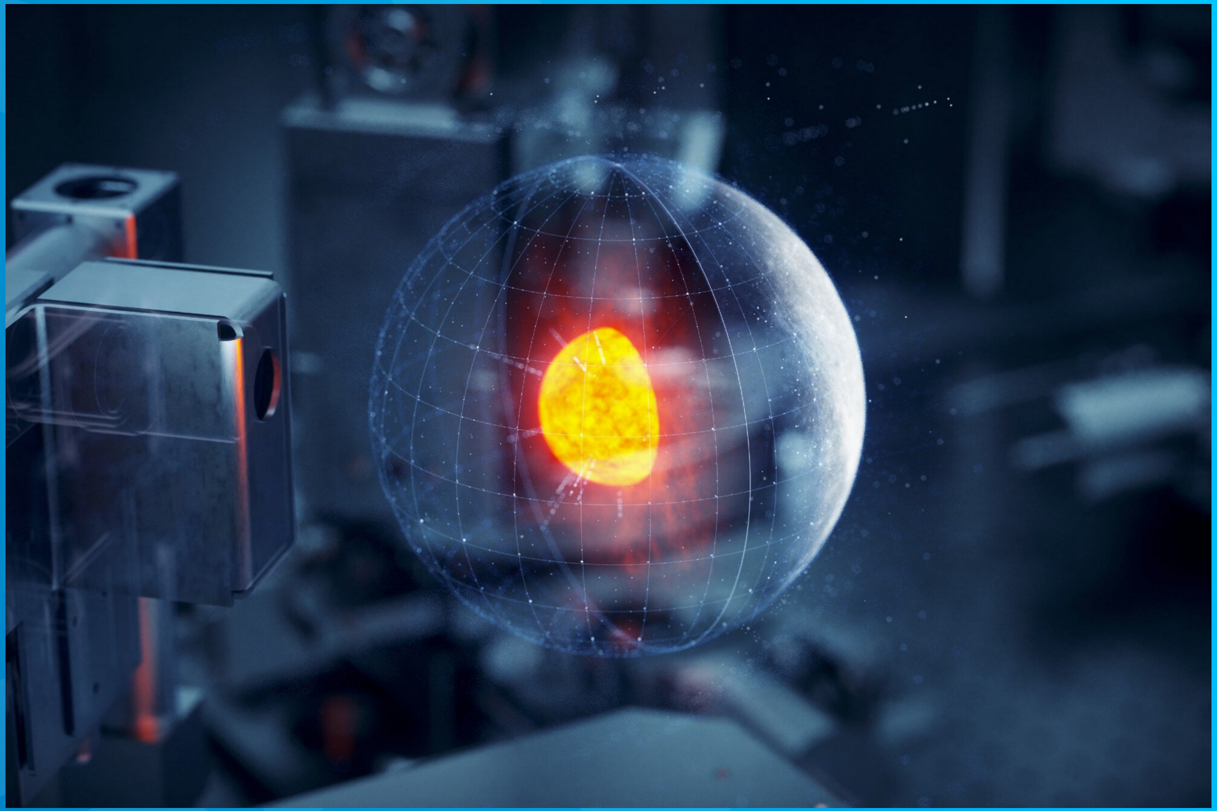

https://www.hzdr.de/db/Cms?pOid=50704&pNid=708

M. Böhme, Z. A. Moldabekov, J. Vorberger, and T.Dornheim Phys. Rev. Lett. 129, 066402 (2022)

Warm Dense Matter

Inertial confinement fusion

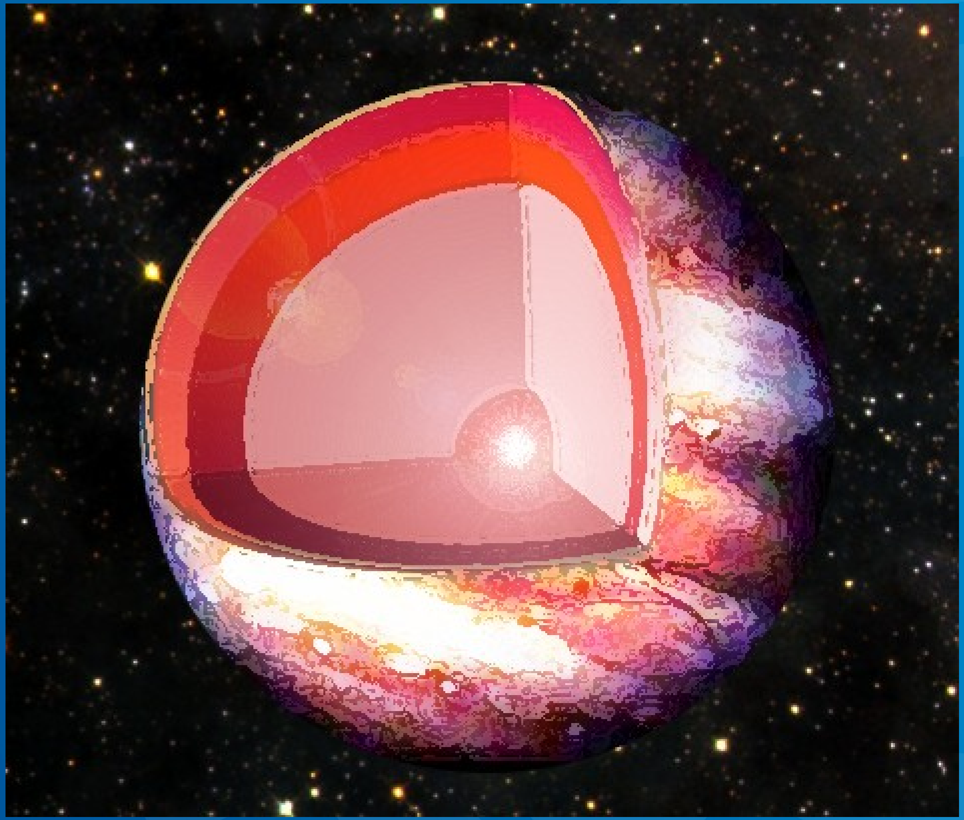

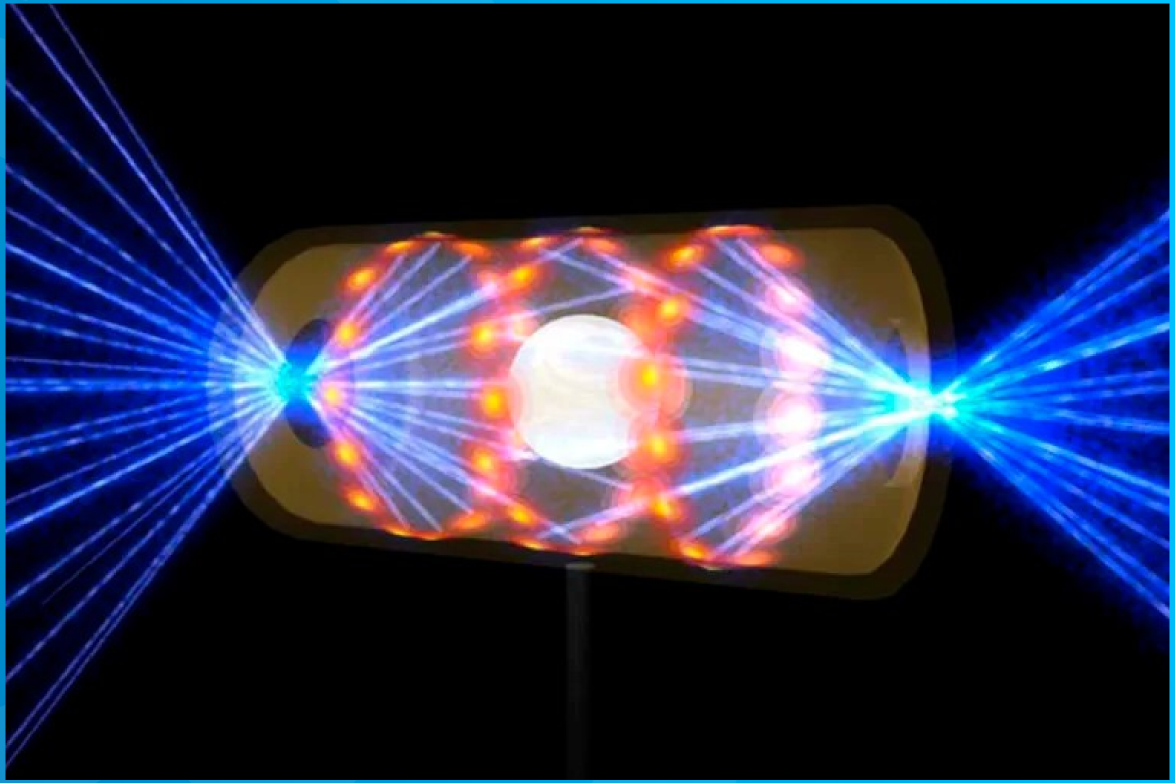

https://newscenter.lbl.gov/2009/10/14/warm-dense-matter/

Warm Dense Matter

CASUS
CENTER FOR ADVANCED SYSTEMS UNDERSTANDING

- The European X-ray Free- Electron Laser (XFEL)
- The National Ignition Facility
- The Linac coherent light source at SLAC
- The Sandia Z-machine

the European XFEL

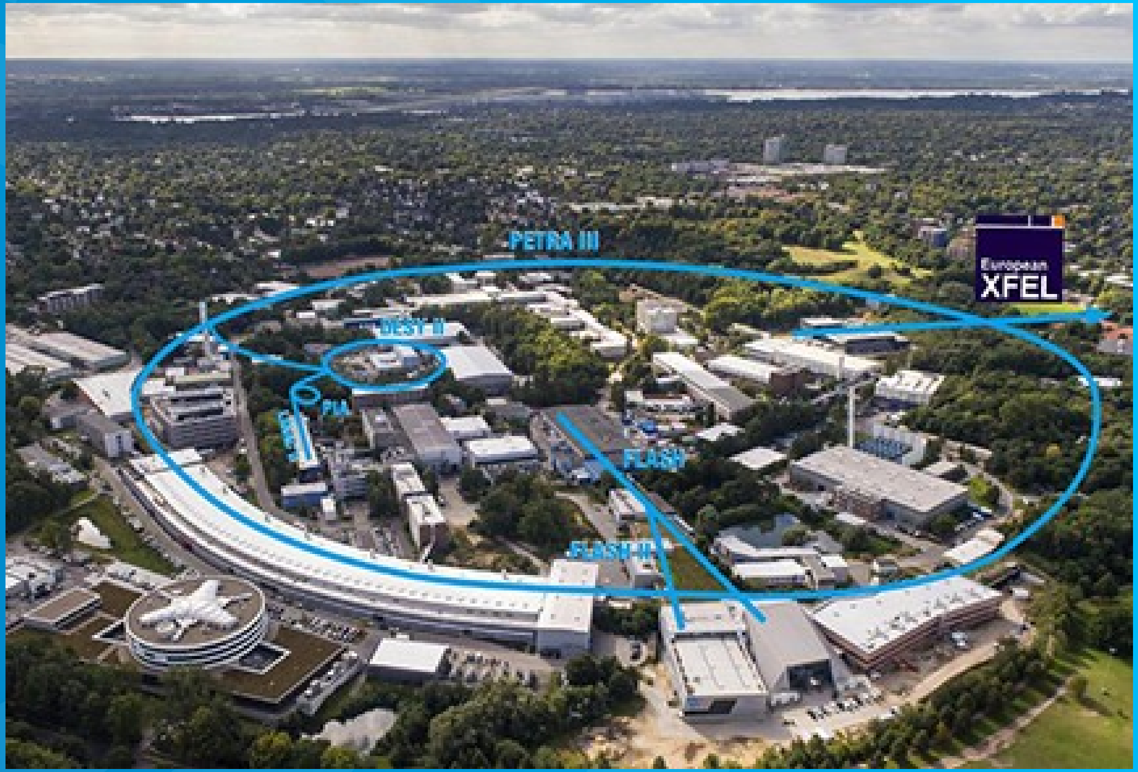

https://photon-science.desy.de

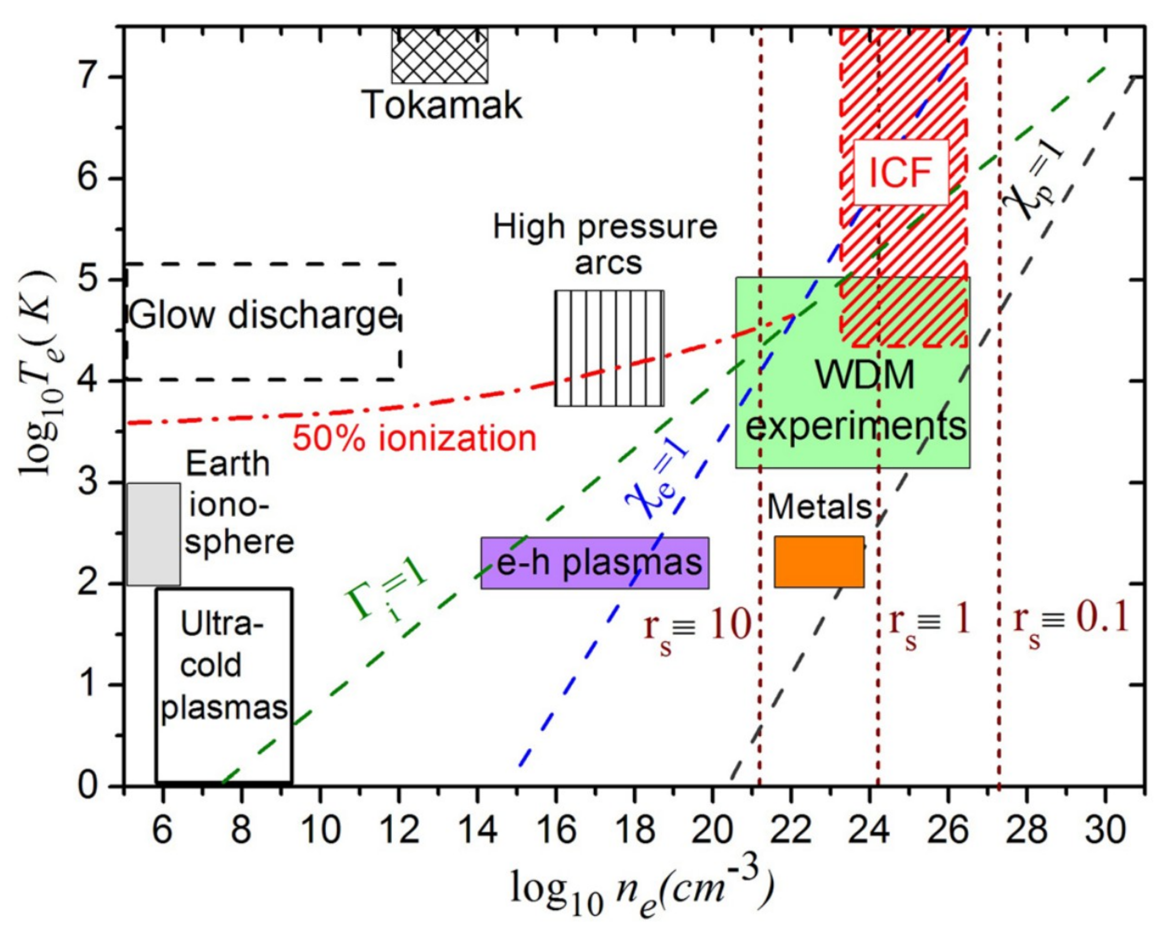

POP 26, 090601 (2019);
also see NRL PLASMA FORMULARY.

Electron coupling parameter:

$$r_s = a_W/a_B$$

Degeneracy parameter:

$$\theta = T/E_F$$

Theoretical Background

Density Functional Theory (DFT)

An electronic Hamiltonian

$$\hat{H} = \hat{T} + \hat{V}_{ee} + \hat{V}$$

$$n(\boldsymbol{r}, t) = \sum_i f_i |\phi_i(\boldsymbol{r}, t)|^2$$

$$i\hbar \frac{\partial}{\partial t} \phi_i(\boldsymbol{r}, t) = \left[-\frac{\hbar^2}{2m} \nabla^2 + v_S(\boldsymbol{r}, t) \right] \phi_i(\boldsymbol{r}, t)$$

$$v_S(\boldsymbol{r}, t) = v(\boldsymbol{r}, t) + v_H[n](\boldsymbol{r}, t) + v_{XC}[n](\boldsymbol{r}, t)$$

Linear density response of electrons in warm dense matter

Dynamic density response function

$$\chi(\mathbf{q},\omega) = \frac{\chi_0(\mathbf{q},\omega)}{1 - \left[v(q) + K_{\mathrm{xc}}(\mathbf{q},\omega)\right]\chi_0(\mathbf{q},\omega)}$$

XC-kernel

a known reference function

χ_0

- **the Lindhard function** → Dense plasmas, uniform electron gas (UEG) model
- **the KS response function** → **LR-TDDFT** simulations of real materials

Applications

the dynamic structure factor, the dielectric properties,

the transport properties, the stopping power ...

Static XC-kernel

$$K_{\mathrm{xc}}(\mathbf{q}) = K_{\mathrm{xc}}(\mathbf{q}, 0)$$

$$K_{\mathrm{xc}}(\mathbf{q}) = -\left\{ v(q) + \left(\frac{1}{\chi(\mathbf{q})} - \frac{1}{\chi_0(\mathbf{q})} \right) \right\}$$

Utility: Dynamic response in the *static approximation*

$$\chi_{\mathrm{stat}}(\mathbf{q}, \omega) = \frac{\chi_0(\mathbf{q}, \omega)}{1 - \left[v(q) + K_{\mathrm{xc}}(\mathbf{q}) \right] \chi_0(\mathbf{q}, \omega)}$$

Computation of the Static Exchange–Correlation Kernel of Real Materials

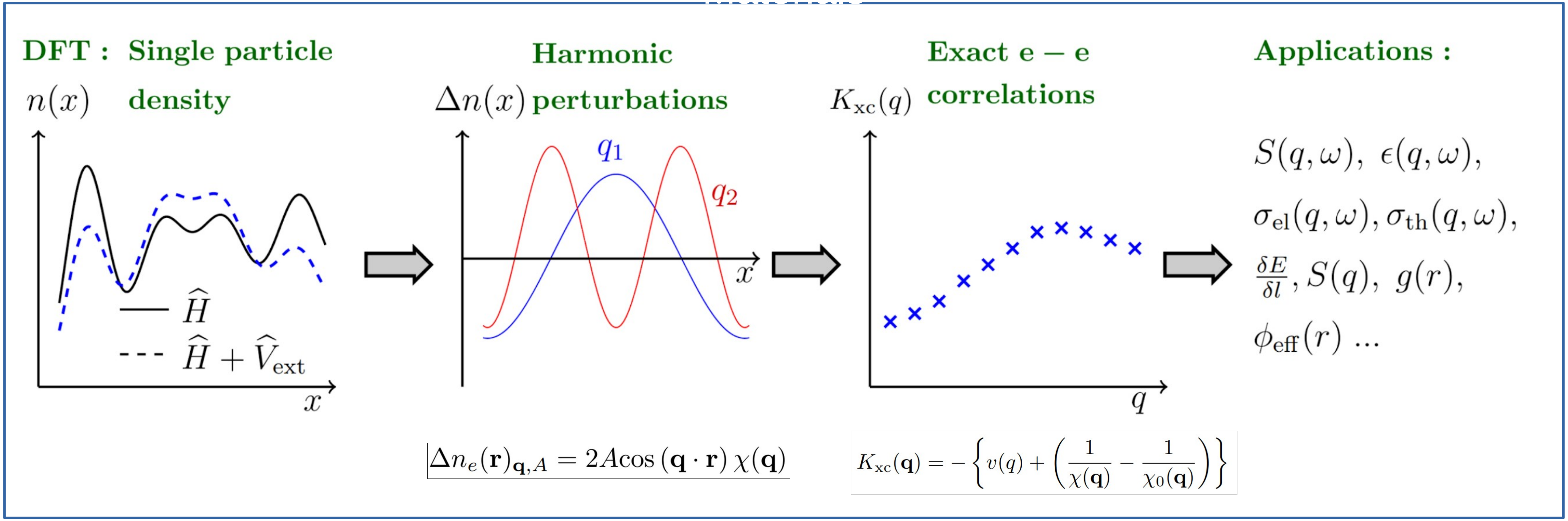

Z. Moldabekov, M. Böhme, J. Vorberger, D. Blaschke, T. Dornheim, **arXiv:2209.00928** (2022)

UEG in the ground state
[low temperature limit]

$$G(\mathbf{q},\omega) = -\frac{1}{v(q)} K_{\mathrm{xc}}(\mathbf{q},\omega)$$

Results from:
Z. Moldabekov, M. Böhme, J. Vorberger,
D. Blaschke, T. Dornheim, **arXiv:2209.00928** (2022)

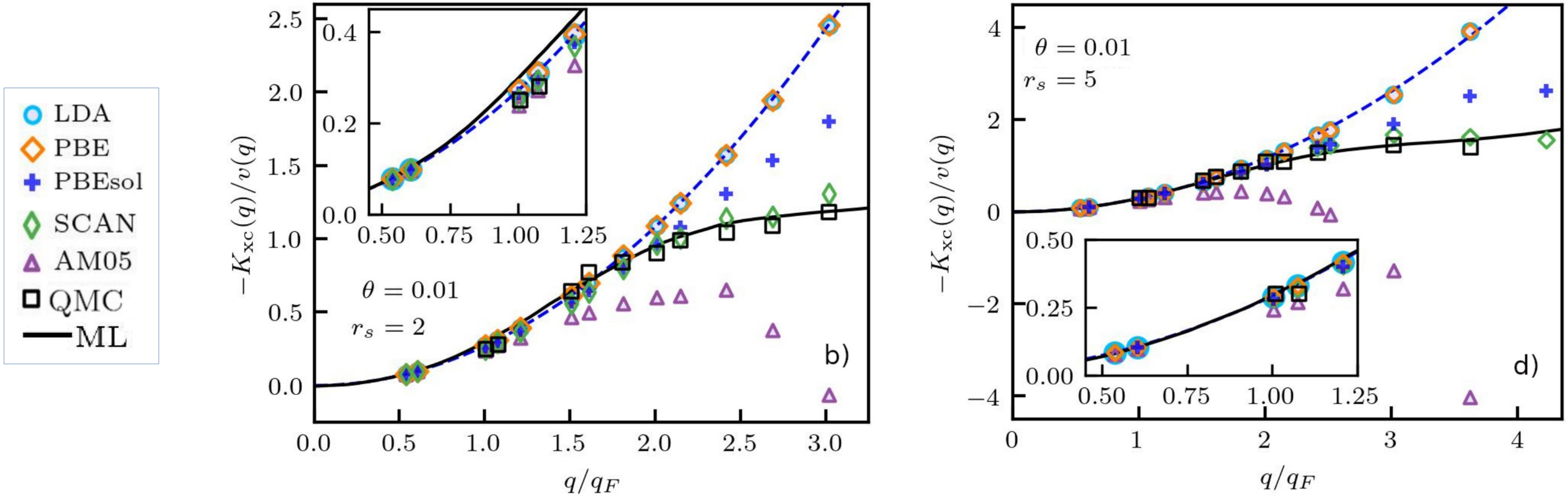

[LDA] J. P. Perdew and Y. Wang, PRB (1992)
[PBE] J. P. Perdew, K. Burke, and M. Ernzerhof, PRL (1996).
[PBEsol] J. P. Perdew et. al., PRL (2008).
[SCAN] J. Sun, A. Ruzsinszky, and J. P. Perdew, PRL (2015).
[ML] **PIMC based parameterization**, see T. Dornheim et. al., JCP (2019)

QMC: S. Moroni et al., Phys. Rev. Lett 75, 689 (1995).

UEG at WDM conditions
[high temperatures]

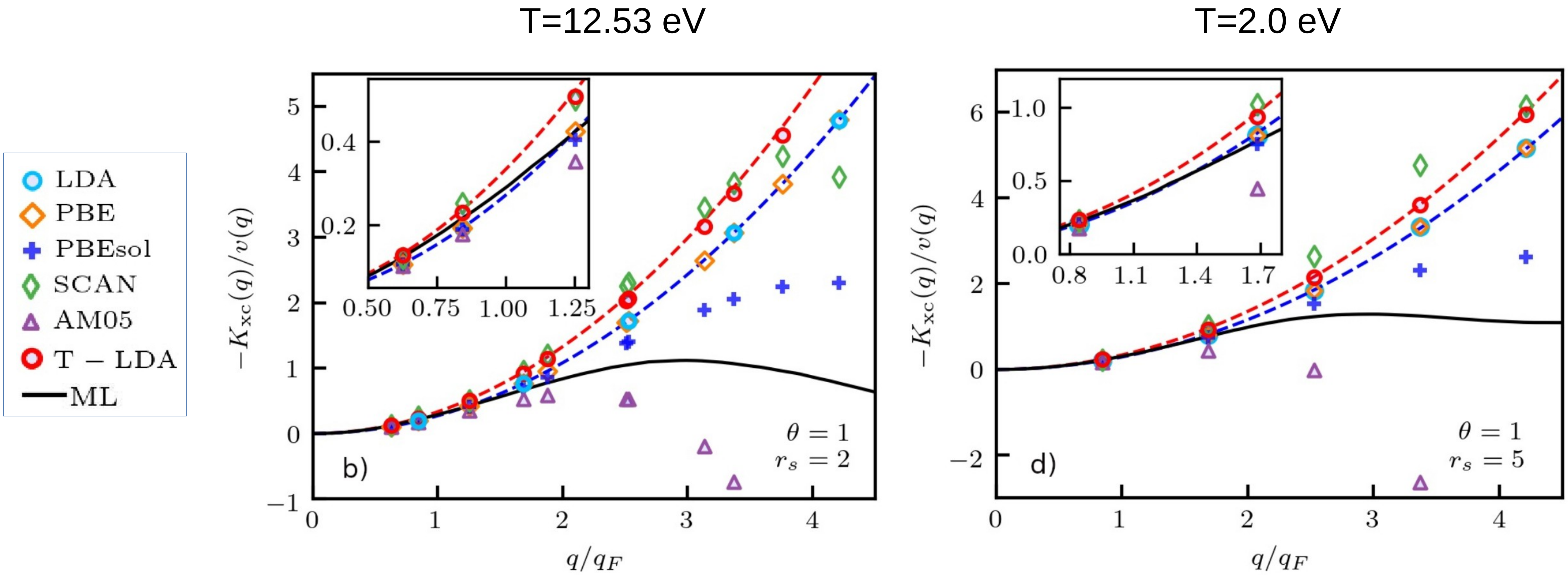

[T-LDA] S. Groth et. al., PRL 119, 135001 (2017)

Results from:
Z. Moldabekov, M. Böhme, J. Vorberger, D. Blaschke, T. Dornheim, **arXiv:2209.00928** (2022)

Finite temperature LDA performs worse than its ground state version !!!

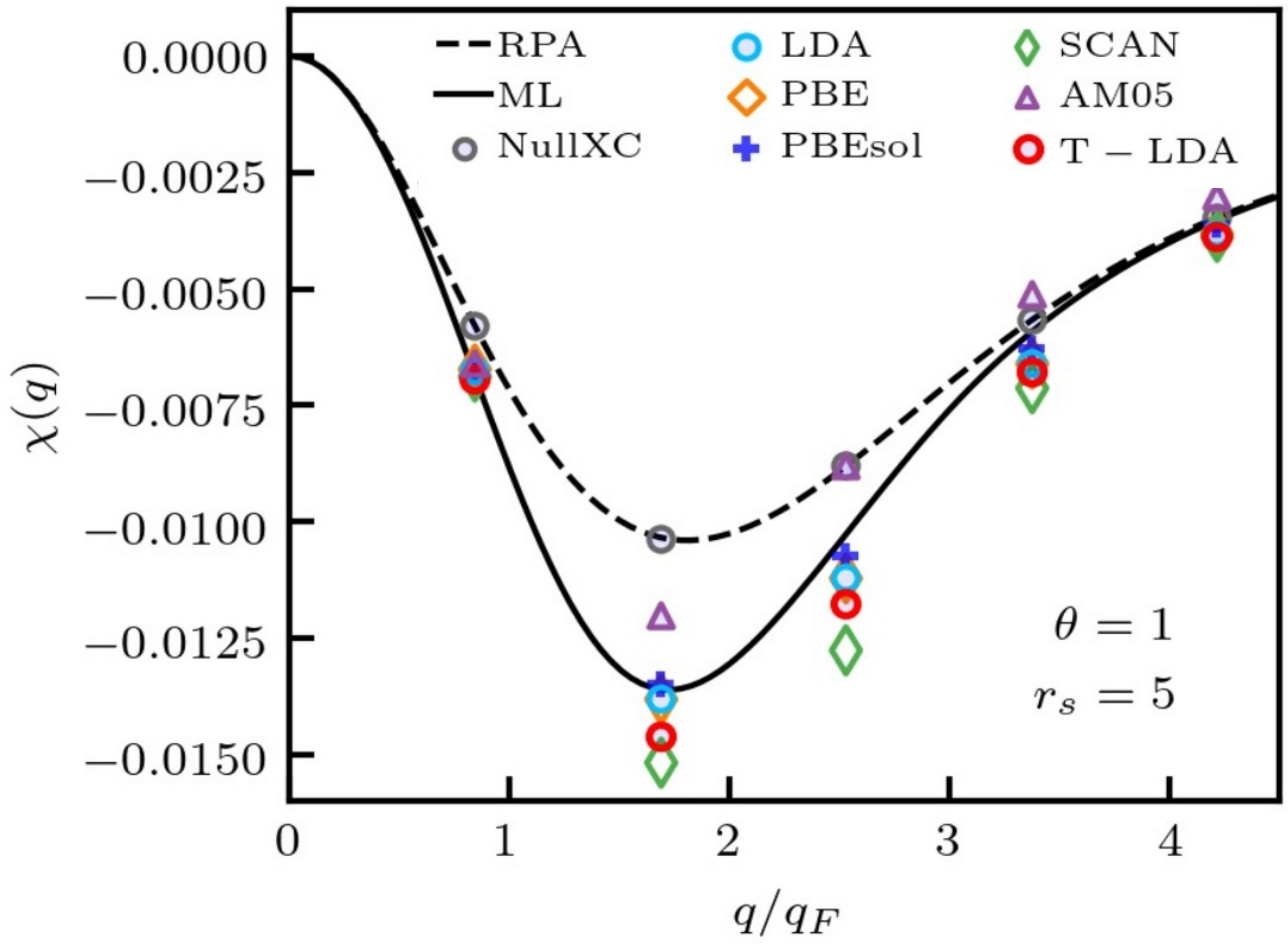

[LDA] J. P. Perdew and Y. Wang, PRB (1992)

[PBE] J. P. Perdew, K. Burke, and M. Ernzerhof, PRL (1996).

[PBEsol] J. P. Perdew et. al., PRL (2008).

[SCAN] J. Sun, A. Ruzsinszky, and J. P. Perdew, PRL (2015).

[T-LDA] S. Groth et. al., PRL 119, 135001 (2017)

[ML] **PIMC based parameterization**, see T. Dornheim et. al., JCP (2019)

Zhandos A. Moldabekov, Maximilian Böhme, Jan Vorberger, David Blaschke, and Tobias Dornheim, **arXiv:2209.00928** (2022)

Relative agreement measure

$$\mathrm{RAM} = \frac{\int_0^{2q_F} |G_{\mathrm{LDA}}(q) - G_{\mathrm{ML}}(q)|\, dq}{\int_0^{2q_F} |G_{\mathrm{T-LDA}}(q) - G_{\mathrm{ML}}(q)|\, dq} = \frac{\Delta_{\mathrm{LDA}}}{\Delta_{\mathrm{T-LDA}}}$$

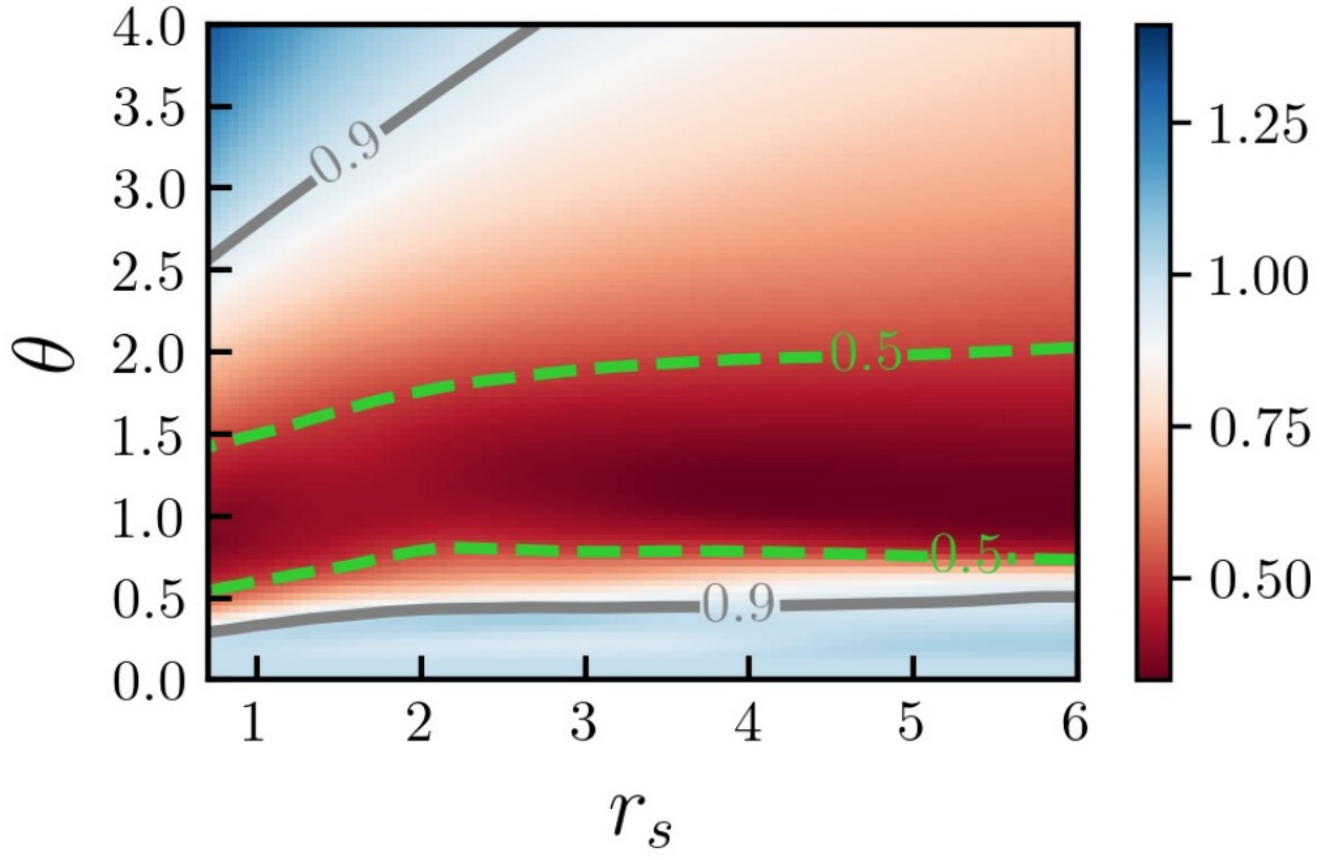

Non-empirical mixing coefficient for hybrid XC functionals

$$E_{\mathrm{xc}}[\rho_\sigma, n] = E_{\mathrm{c}}^{\mathrm{DF}}[n] + aE_x^{\mathrm{HF}}[\rho_\sigma] + (1-a)E_{\mathrm{x}}^{\mathrm{DF}}[n]$$

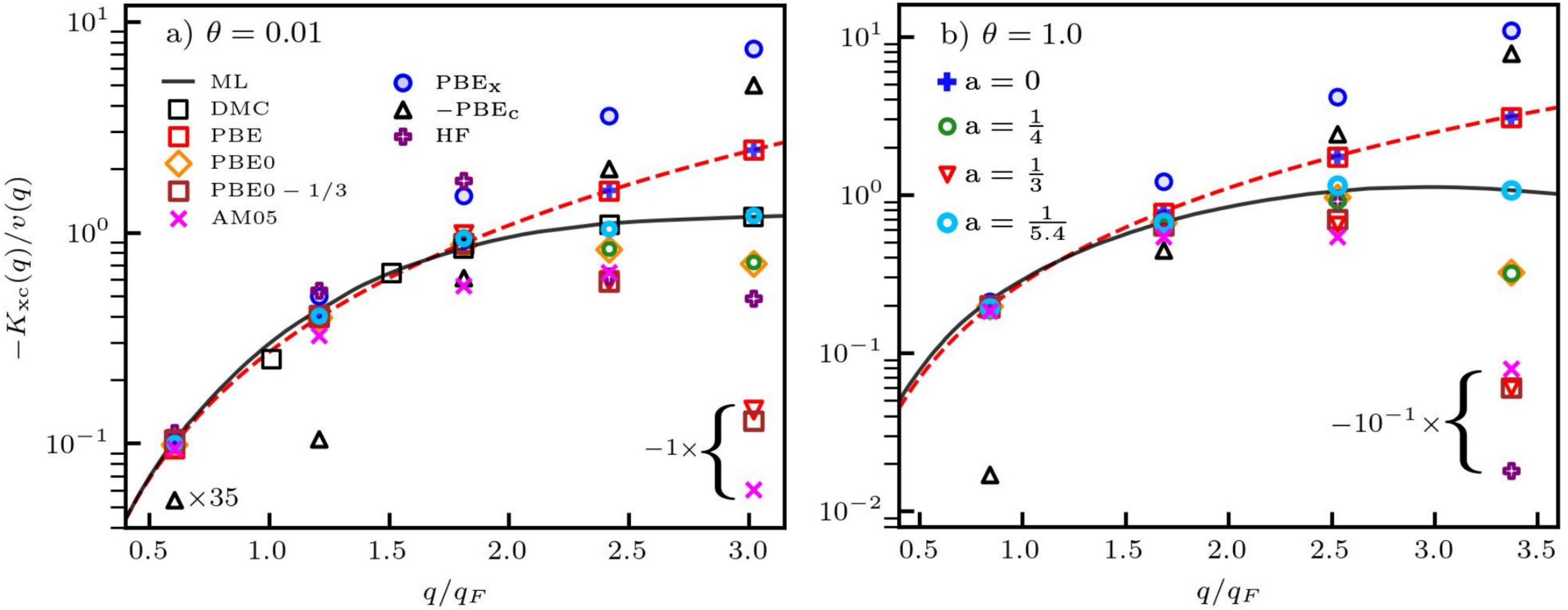

Zhandos A. Moldabekov, Mani Lokamani, Jan Vorberger, Attila Cangi, Tobias Dornheim, arXiv:2212.00644 (2022)

Non-empirical mixing coefficient for hybrid XC functionals

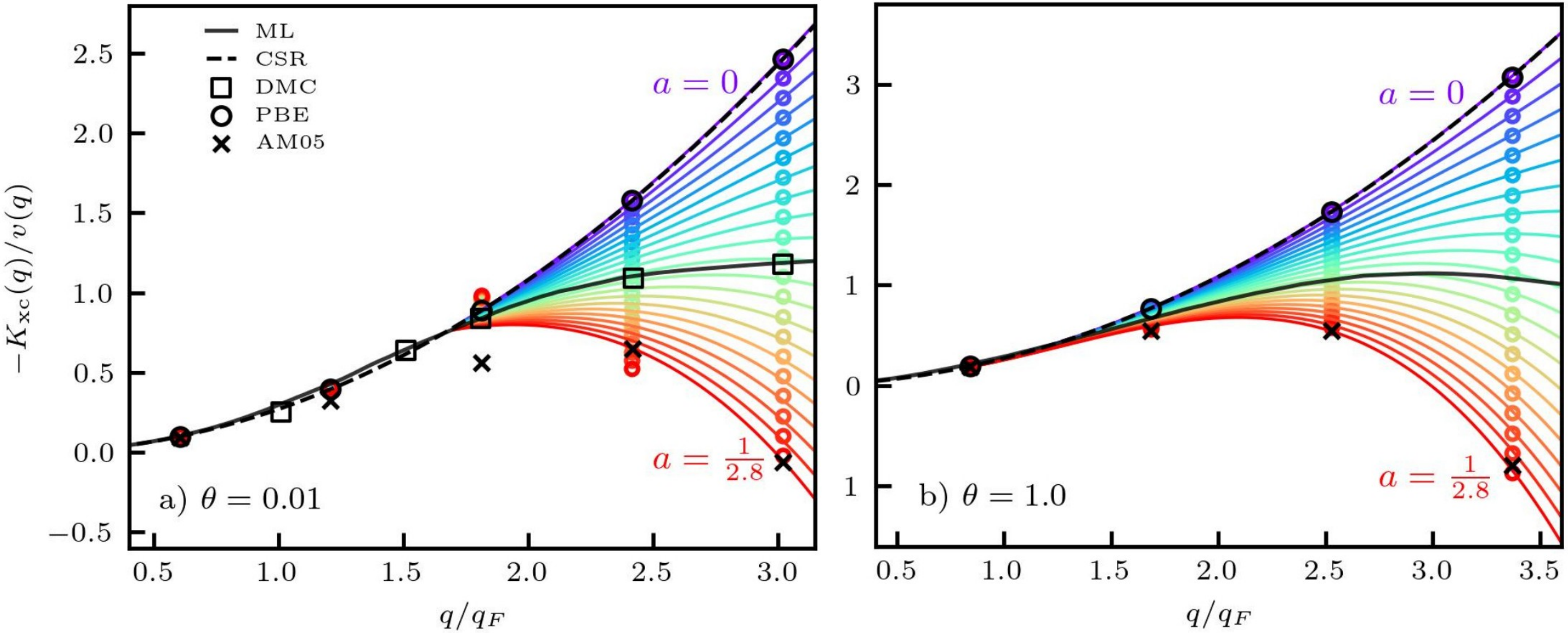

Zhandos A. Moldabekov, Mani Lokamani, Jan Vorberger, Attila Cangi, Tobias Dornheim,
arXiv:2212.00644 (2022)

WDM Hydrogen

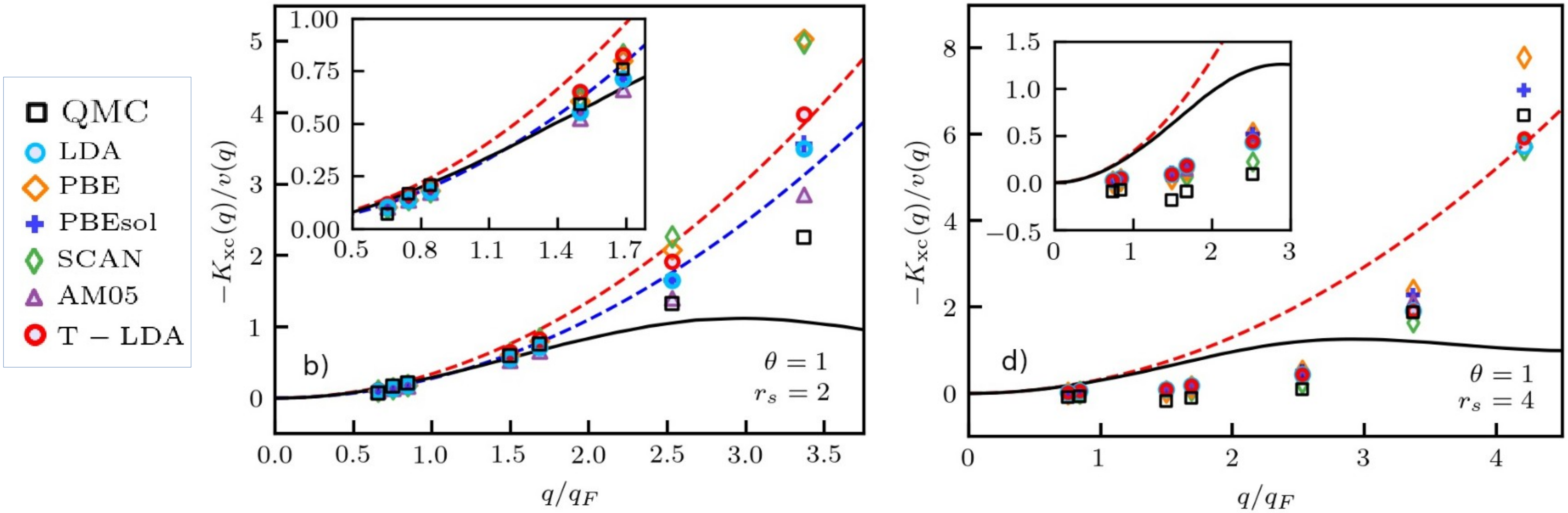

QMC data from:
M Boehme, Z. Moldabekov, J. Vorberger, and
T. Dornheim, Phys. Rev. Lett. **129**, 066402 (2022).

Results from:
Z. Moldabekov, M. Böhme, J. Vorberger,
D. Blaschke, T. Dornheim, **arXiv:2209.00928** (2022)

Conclusions:

1. We have presented a new approach to compute the electronic static XC-kernel of any given material within the framework of DFT, and without any additional external input apart from the usual XC-functional.

2. We have found that the ground-state LDA/PBE functionals perform better than their consistently temperature-dependent counterparts at WDM conditions.

3. We have found that the DFT calculations are capable to very accurately describe the static XC-kernel and density response of warm dense hydrogen.

4. The material-specific static XC-kernel with the consistent dynamic KS reference function provides the basis for the systematic development of future LR-TDDFT calculations of various dynamic, structural, and transport properties of electrons

Reference:

Z. Moldabekov, M. Böhme, J. Vorberger, D. Blaschke, T. Dornheim, **arXiv:2209.00928** (2022)

Non-linear density response of electrons in warm dense matter

Probing WDM to measure response

S. Moroni, D. M. Ceperley, and G. Senatore, PRL 69, 1837 (1992)

$$\hat{H} = \hat{H}_{\text{UEG}} + 2\,A \sum_{i}^{N} \cos(\boldsymbol{r}_i \cdot \boldsymbol{q})$$

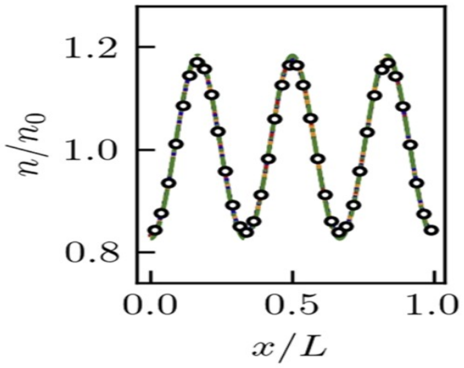

Linear response regime: $\delta n(\mathbf{r}) = 2\,A \cos(\boldsymbol{r} \cdot \boldsymbol{q}) \chi(\mathbf{q})$ ⟷ $|\delta n_(\mathbf{r})|/n_0 \ll 1$

General non-linear response result:

$$\delta n(\mathbf{r}) = 2\,\rho^{(1)} \cos(\boldsymbol{r} \cdot \boldsymbol{q}) + 2\,\rho^{(2)} \cos(\boldsymbol{r} \cdot 2\boldsymbol{q}) + 2\,\rho^{(3)} \cos(\boldsymbol{r} \cdot 3\boldsymbol{q}) + \ldots$$

Linear static density response function for $r_s = 2$

$$\delta n(\mathbf{r}) = 2\,A\cos(\boldsymbol{r}\cdot\boldsymbol{q})\chi(\mathbf{q})$$

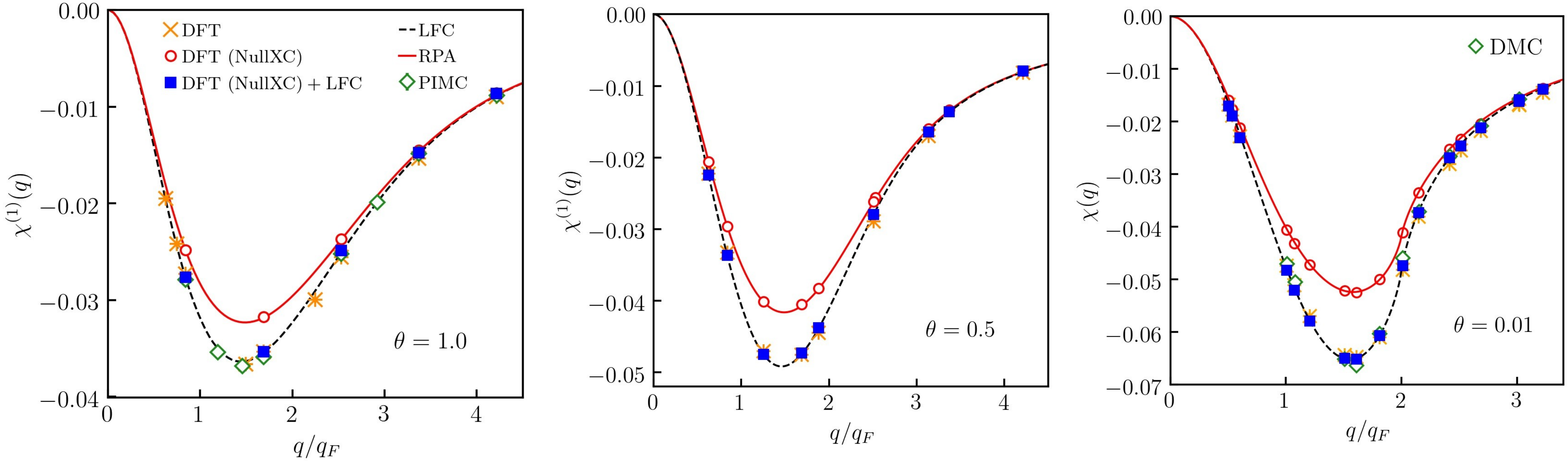

Zhandos Moldabekov, Jan Vorberger, Tobias Dornheim, **J. Chem. Theory Comput**. 18, 5, 2900–2912 (2022)

DMC data: **S. Moroni, D. M. Ceperley, and G. Senatore, PRL 75, 689 (1995)**

Quadratic

$$\rho^{(2)} = \chi^{(2)}(\mathbf{q})\ A^2$$

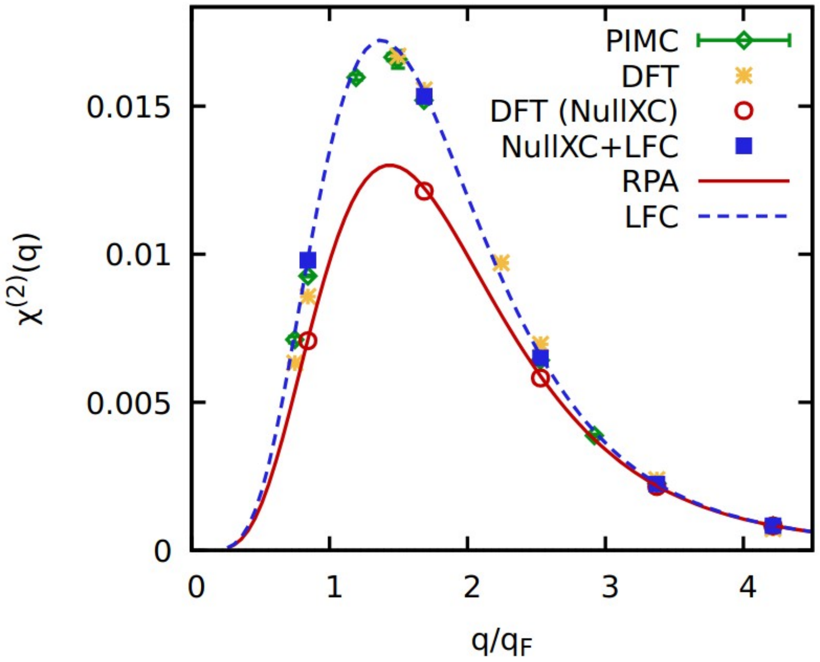

Cubic

$$\rho^{(1)} = \chi^{(1)}(\mathbf{q})\ A + \chi^{(1,\mathrm{cubic})}(\mathbf{q})\ A^3$$

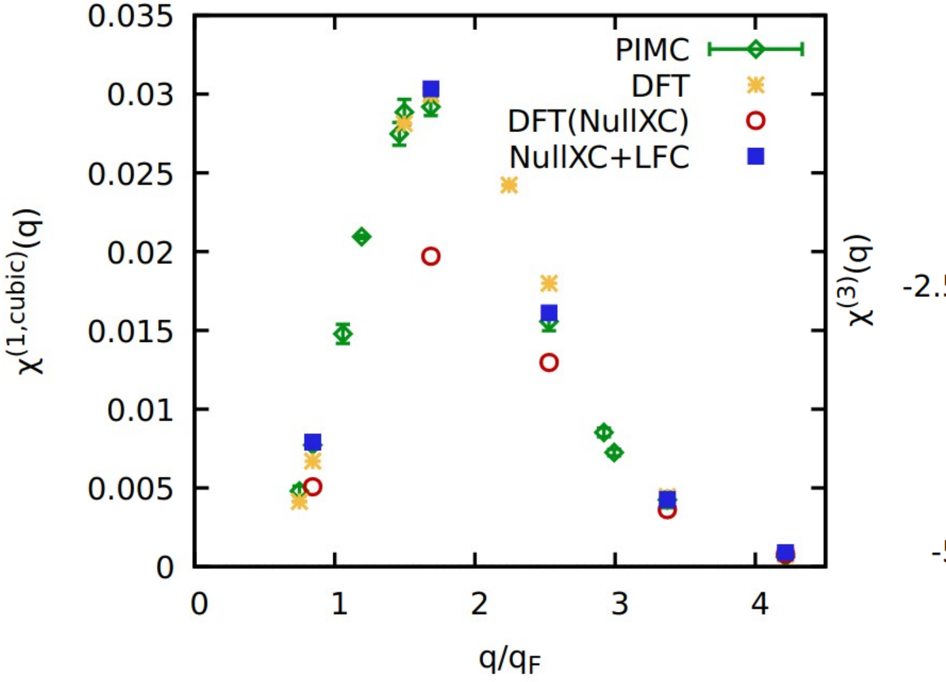

Cubic

$$\rho^{(3)} = \chi^{(3)}(\mathbf{q})\ A^3$$

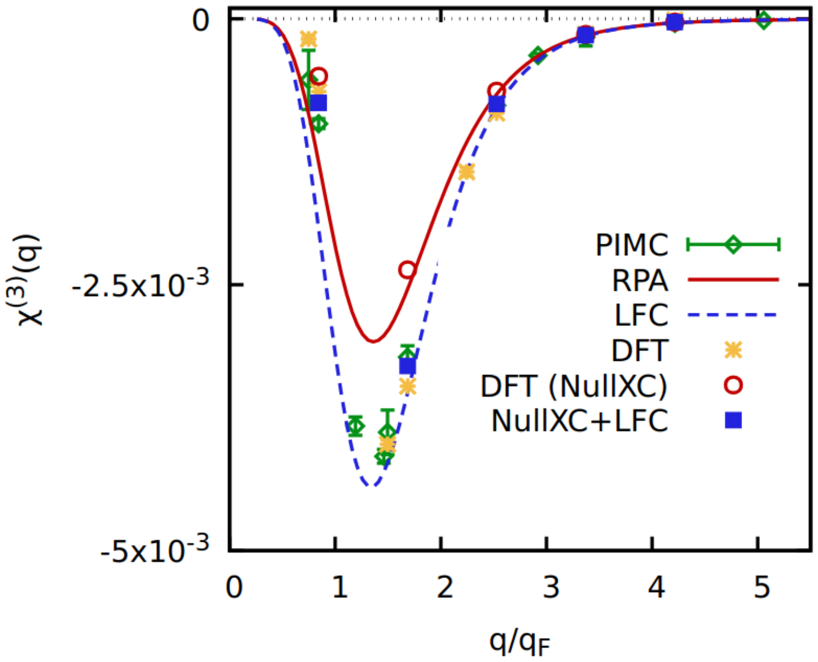

$r_s = 2$ and $\theta = 1$

DFT data: Zhandos Moldabekov, Jan Vorberger, Tobias Dornheim, **J. Chem. Theory Comput**. 18, 5, 2900–2912 (2022)

Theory: S. A. Mikhailov, **PRL** 113, 027405 (2014).

PIMC data: T. Dornheim, M. Böhme, Z. A. Moldabekov, J. Vorberger, and M. Bonitz, **PRR** 3, 033231 (2021)

Applications of a newly developed method based on KS-DFT:

1. Development of Kinetic Energy Functionals for OF-DFT and TD-OFDFT
   [can now be material specific !]

2. Guide theoretical development of Nonlinear-LRT

3. Nonlinear response of complex materials

JCTC Journal of Chemical Theory and Computation

pubs.acs.org/JCTC Article

Density Functional Theory Perspective on the Nonlinear Response of Correlated Electrons across Temperature Regimes

Zhandos Moldabekov,* Jan Vorberger, and Tobias Dornheim

Cite This: *J. Chem. Theory Comput.* 2022, 18, 2900–2912 Read Online

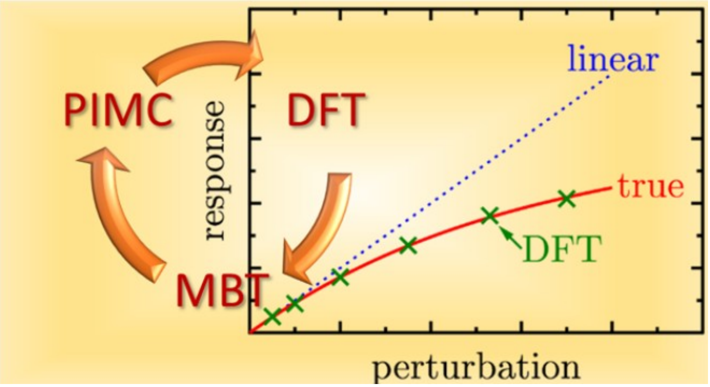

Developing Quantum Fluid Theory of Electrons from First Principles

Single particle limit

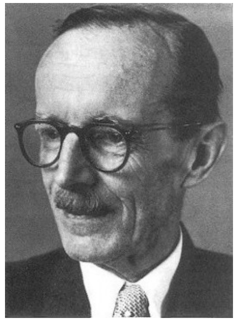

E. Madelung,
Z. Phys. (1927)

D. Bohm,
Phys. Rev. (1952)

$$\Psi(\mathbf{R},t) = A(\mathbf{R},t)\, e^{\frac{i}{\hbar}S(\mathbf{R},t)}$$

↓

$$i\hbar\frac{\partial\Psi(\mathbf{R},t)}{\partial t} = \hat{H}\Psi(\mathbf{R},t)$$

→

$$n(\mathbf{r},t) = A^2(\mathbf{r},t), \qquad \text{density},$$

$$\mathbf{p}(\mathbf{r},t) = m\mathbf{v}(\mathbf{r},t) = \nabla S(\mathbf{r},t), \quad \text{momentum},$$

↓

$$\frac{\partial n}{\partial t} + \nabla(\mathbf{v}n) = 0,$$

$$\frac{\partial \mathbf{p}}{\partial t} + \mathbf{v}\nabla\mathbf{p} = -\nabla(V+Q),$$

"Bohm potential"

$$Q[n(\mathbf{r},t)] = -\frac{\hbar^2}{2m}\frac{\nabla^2 n^{1/2}}{n^{1/2}},$$

$$m\frac{d}{dt}\vec{v} = -\nabla(V+Q)$$

Many-electron system:

Microscopic picture of Fermi fluid

Step 1. We start from a set of N time-dependent Kohn-Sham (KS) equations:

$$i\hbar\frac{\partial}{\partial t}\phi_i(\boldsymbol{r},t) = \left[-\frac{\hbar^2}{2m}\nabla^2 + v_{\mathrm{S}}(\boldsymbol{r},t)\right]\phi_i(\boldsymbol{r},t)$$

$$v_{\mathrm{S}}(\boldsymbol{r},t) = v(\boldsymbol{r},t) + v_{\mathrm{H}}[n](\boldsymbol{r},t) + v_{\mathrm{XC}}[n](\boldsymbol{r},t)$$

Step 1. We start from a set of N time-dependent Kohn-Sham (KS) equations

$$i\hbar\frac{\partial}{\partial t}\phi_i(\boldsymbol{r},t) = \left[-\frac{\hbar^2}{2m}\nabla^2 + v_S(\boldsymbol{r},t)\right]\phi_i(\boldsymbol{r},t)$$

$$v_S(\boldsymbol{r},t) = v(\boldsymbol{r},t) + v_H[n](\boldsymbol{r},t) + v_{XC}[n](\boldsymbol{r},t)$$

Step 2. The amplitude-phase representation of the KS orbitals

$$\phi_i(\boldsymbol{r},t) = \sqrt{n_i(\boldsymbol{r},t)}\exp\left[iS_i(\boldsymbol{r},t)\right]$$

$$\mathbf{v}_i = \nabla S_i/m,$$

Step 1. We start from a set of N time-dependent Kohn-Sham (KS) equations

$$i\hbar\frac{\partial}{\partial t}\phi_i(\boldsymbol{r},t) = \left[-\frac{\hbar^2}{2m}\nabla^2 + v_{\mathrm{S}}(\boldsymbol{r},t)\right]\phi_i(\boldsymbol{r},t)$$

$$v_{\mathrm{S}}(\boldsymbol{r},t) = v(\boldsymbol{r},t) + v_{\mathrm{H}}[n](\boldsymbol{r},t) + v_{\mathrm{XC}}[n](\boldsymbol{r},t)$$

Step 2. The amplitude-phase representation of the KS orbitals

$$\phi_i(\boldsymbol{r},t) = \sqrt{n_i(\boldsymbol{r},t)}\exp\left[iS_i(\boldsymbol{r},t)\right]$$

$$\mathbf{v}_i = \nabla S_i/m,$$

Result: *Microscopic quantum hydrodynamics* (MQHD)

$$\frac{\partial n_i}{\partial t} + \nabla\cdot(n_i\mathbf{v}_i) = 0,$$

$$m\left[\frac{\partial \mathbf{v}_i}{\partial t} + (\mathbf{v}_i\cdot\nabla)\mathbf{v}_i\right] = -\nabla v_{\mathrm{S}} - \nabla\left(-\frac{\hbar^2}{2m}\frac{\nabla^2\sqrt{n_i}}{\sqrt{n_i}}\right)$$

MQHD is equivalent to TD-DFT

Coarse-grained models for quantum fluid

MQHD

CASUS
CENTER FOR ADVANCED SYSTEMS UNDERSTANDING

$$\frac{\partial n_i}{\partial t} + \nabla \cdot (n_i \mathbf{v}_i) = 0,$$

$$m\left[\frac{\partial \mathbf{v}_i}{\partial t} + (\mathbf{v}_i \cdot \nabla)\mathbf{v}_i\right] = -\nabla v_S - \nabla\left(-\frac{\hbar^2}{2m}\frac{\nabla^2\sqrt{n_i}}{\sqrt{n_i}}\right)$$

$$\bar{n}(\boldsymbol{r},t) = \sum_i f_i n_i(\boldsymbol{r},t)/N$$

$$\mathbf{v} = \sum_i f_i \mathbf{v}_i/N$$

$$\mathbf{E} = -\nabla\left[v + v_{\mathrm{H}}\right]$$

$$P_e = \frac{1}{2m}\partial_\alpha \overline{\delta p_{i\alpha}^2}$$

$$\boldsymbol{\sigma}_e = \frac{1}{m}\partial_\gamma \overline{\delta p_{i\alpha}\delta p_{i\gamma}}$$

The many-fermion Bohm potential

$$\tilde{v}_B(\boldsymbol{r},t) = -\frac{\hbar^2}{2mN}\sum_{i=1}^{N} f_i \frac{\nabla^2\sqrt{n_i(\boldsymbol{r},t)}}{\sqrt{n_i(\boldsymbol{r},t)}}$$

$$\frac{\partial \bar{n}}{\partial t} + \frac{1}{N}\sum_i f_i \nabla \cdot (n_i \mathbf{v}_i) = 0$$

$$m\frac{\partial \mathbf{v}}{\partial t} = -\nabla\tilde{v}_B - \frac{1}{n}\nabla P_e + \frac{1}{n}\nabla\cdot\boldsymbol{\sigma}_e + e\mathbf{E} - \nabla v_{\mathrm{XC}}$$

Quantum Fluid Equations

The many-fermion Bohm potential

$$\tilde{v}_B(\boldsymbol{r},t) = -\frac{\hbar^2}{2mN}\sum_{i=1}^{N} f_i \frac{\nabla^2\sqrt{n_i(\boldsymbol{r},t)}}{\sqrt{n_i(\boldsymbol{r},t)}}$$

Previously used approximation:

$$\sum_{i=1}^{N} f_i \frac{\nabla^2\sqrt{n_i(\boldsymbol{r},t)}}{\sqrt{n_i(\boldsymbol{r},t)}} \Longrightarrow \left[\frac{\nabla^2\sqrt{n(\boldsymbol{r},t)}}{\sqrt{n(\boldsymbol{r},t)}}\right]$$

Standard Bohm potential

- For Bose particles in the condensate, the exactness of the standard Bohm potential is proven.
- For fermionic systems, such a proof does not exist.

Investigating the many-fermion Bohm potential

The Bohm potential for a many-fermion system

based on first-principles data from QMC and KS-DFT.

$$\hat{H} = \hat{H}_{\mathrm{UEG}} + \sum_{i=1}^{N} 2A\cos(\boldsymbol{r}_i \cdot \boldsymbol{q})$$

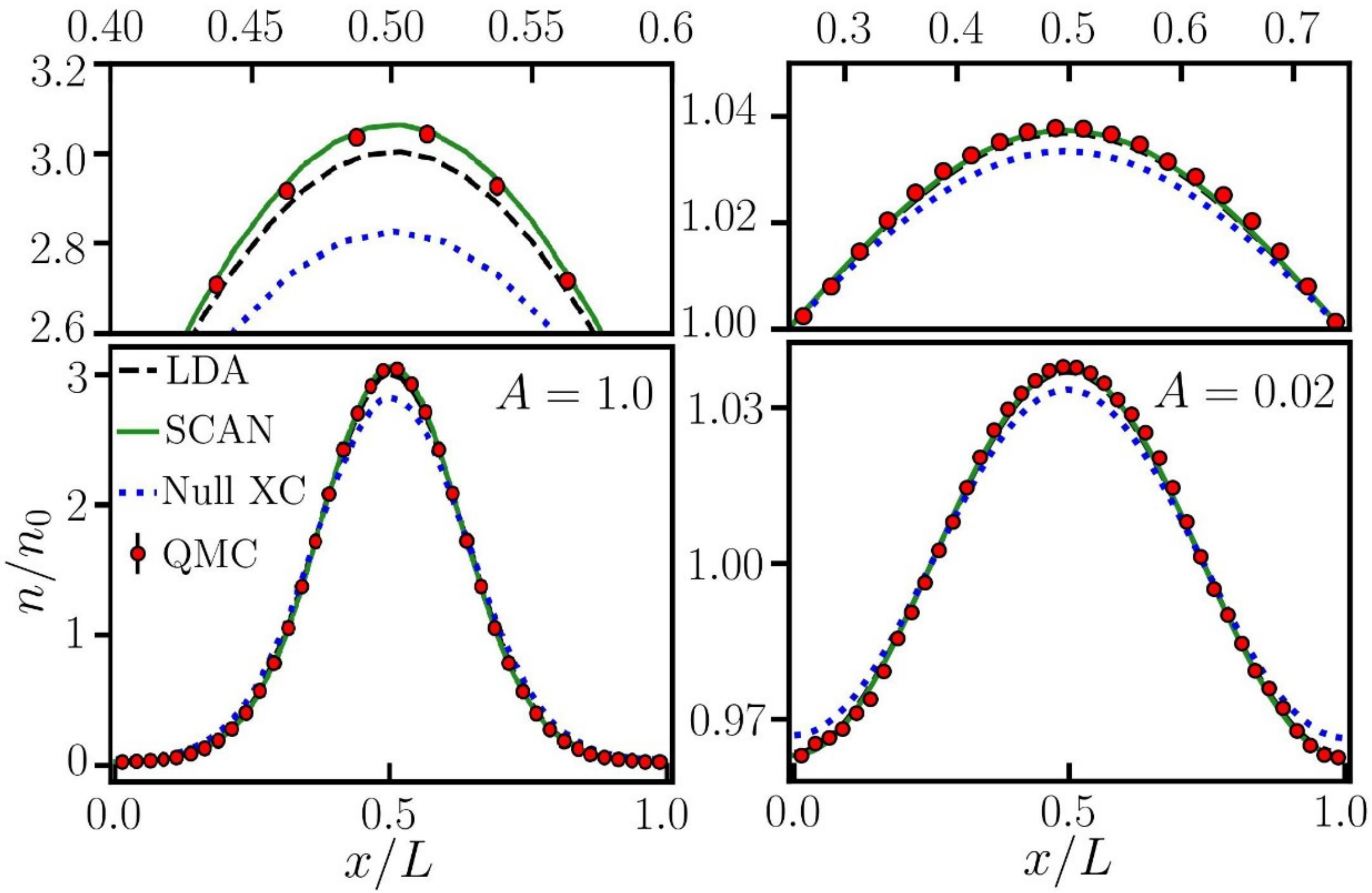

$\theta = k_B T / E_F$

$r_s = a/a_B$

$r_s = 2$ and $\theta = 1$.

The many-fermion Bohm potential

$$\tilde{v}_B(\boldsymbol{r},t) = -\frac{\hbar^2}{2mN}\sum_{i=1}^{N} f_i \frac{\nabla^2\sqrt{n_i(\boldsymbol{r},t)}}{\sqrt{n_i(\boldsymbol{r},t)}}$$

Standard Bohm potential

$$v_B(\boldsymbol{r},t) = -\hbar^2/(2m)\left[\nabla^2\sqrt{n(\boldsymbol{r},t)}/\sqrt{n(\boldsymbol{r},t)}\right]$$

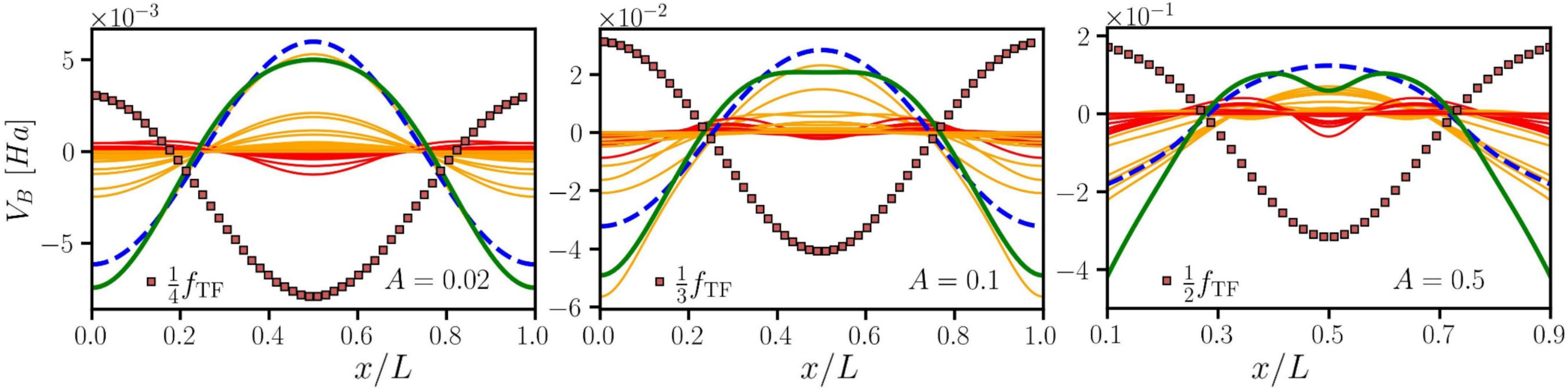

The many-fermion Bohm potential

$$\tilde{v}_B(\boldsymbol{r},t) = -\frac{\hbar^2}{2mN}\sum_{i=1}^{N} f_i \frac{\nabla^2\sqrt{n_i(\boldsymbol{r},t)}}{\sqrt{n_i(\boldsymbol{r},t)}}$$

Standard Bohm potential

$$v_B(\boldsymbol{r},t) = -\hbar^2/(2m)\left[\nabla^2\sqrt{n(\boldsymbol{r},t)}/\sqrt{n(\boldsymbol{r},t)}\right]$$

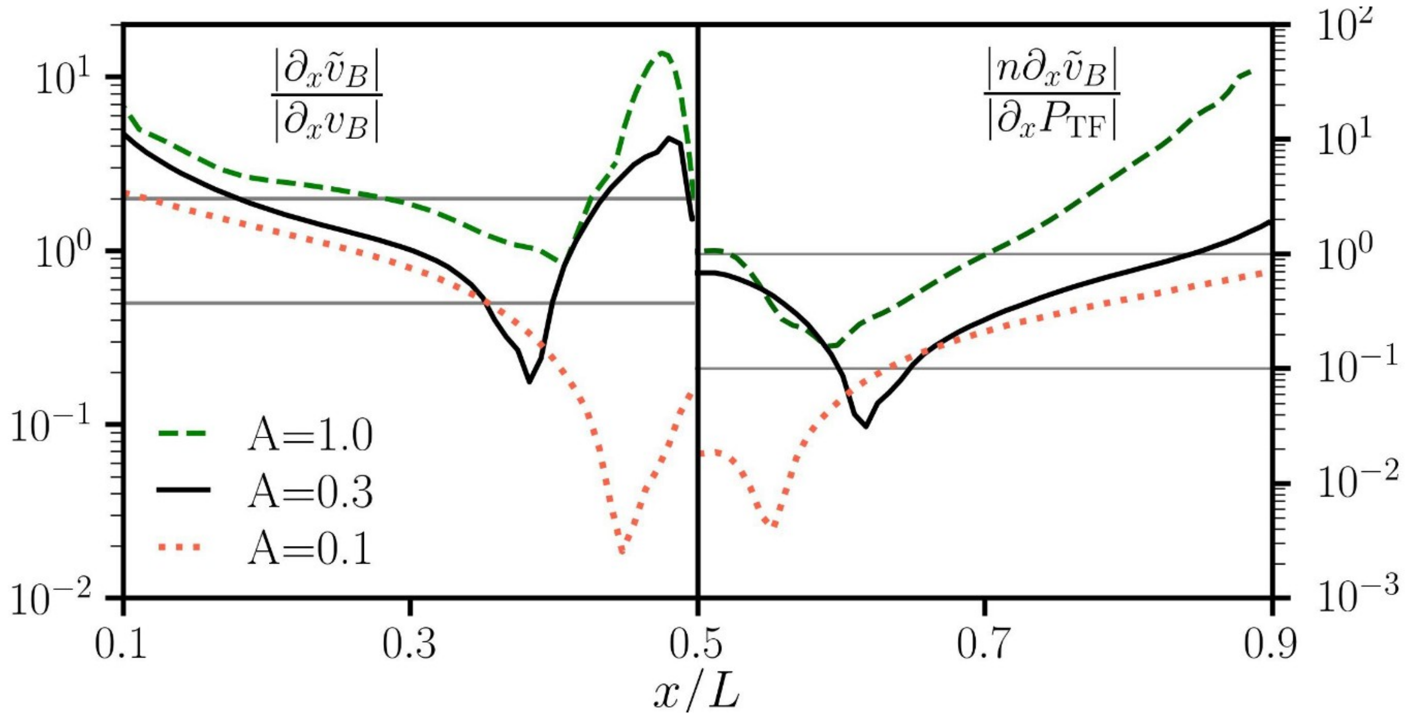

Z. **Moldabekov**, T. Dornheim, G. Gregori, F. Graziani, M. Bonitz, A. Cangi, ***SciPost Physics*** *12, 062 (2022)*

Shock propagation in a quantum electron gas

$$\frac{\partial n}{\partial t} + \left(\frac{\partial nv}{\partial x}\right) = 0,$$

$$\frac{\partial nv}{\partial t} + \left(\frac{\partial nv^2}{\partial x}\right) = -\frac{1}{m}\frac{\partial}{\partial x}\left(P_e + P_Q + P_X\right) + \frac{en}{m}\frac{\partial \phi}{\partial x} + \beta\frac{\partial^2 v}{\partial x^2}.$$

$$P_e = \hbar^2 \frac{\left(3\pi^2\right)^{2/3} n^{5/3}}{5m}$$

$$\frac{\partial^2 \phi}{\partial x^2} = -4\pi e\left(n - n_{ion}\right)$$

$$P_X = -\left(\frac{3}{\pi}\right)^{1/3} \frac{e^2 n^{4/3}}{4}$$

$$P_Q = -\gamma \frac{\hbar^2}{4m} n \frac{\partial^2 \log(n)}{\partial x^2}.$$

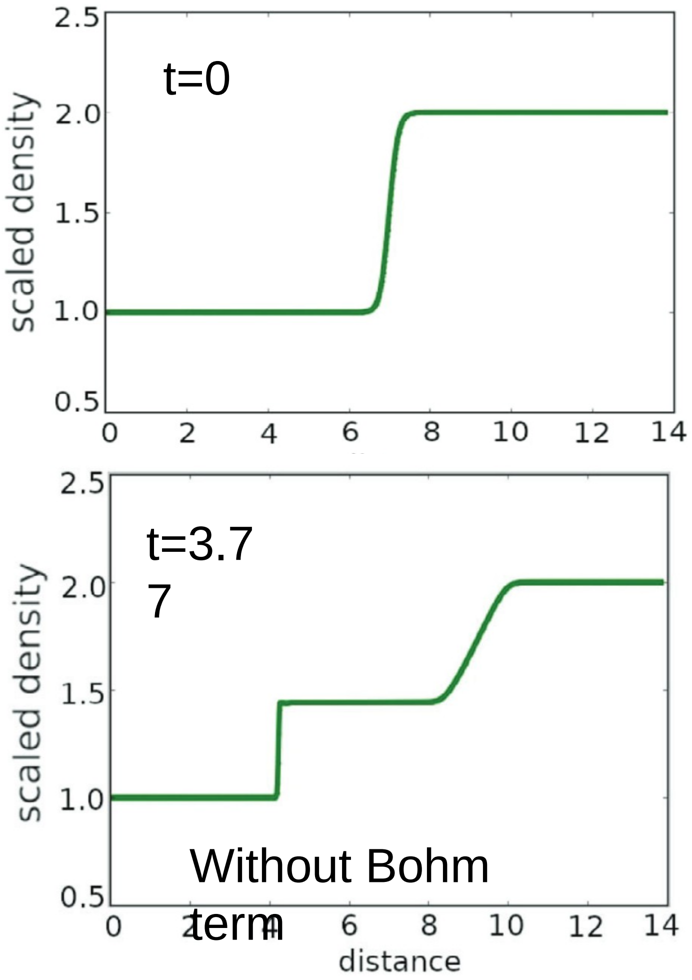

Units: velocity density distance time

$$\varepsilon(\xi,\tau) = v(x,t)/v_{F_0} \quad \eta(\xi,\tau) = n(x,t)V_B r_s^3, \quad \xi = x/\sqrt{3}\lambda_{F_0} \quad t_s = (a_B/c_s). \quad c_s = \left(\frac{5}{3}\frac{P_t}{mn_t}\right)^{1/2}$$

Red lines: Thomas–Fermi pressure, **blue**: exchange pressure, **purple**: the Bohm pressure.

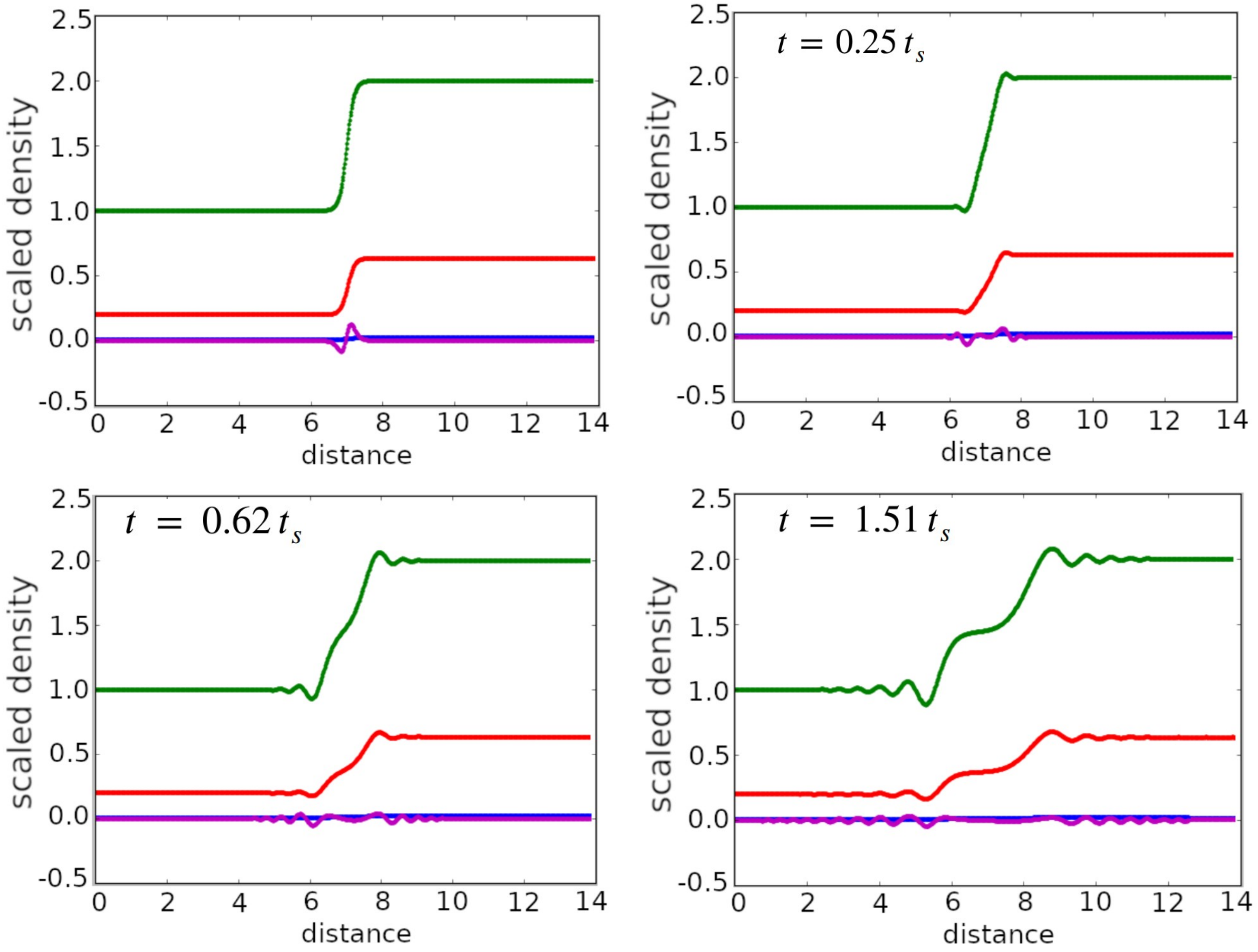

$$\xi = x/\sqrt{3}\lambda_{F_0},$$

$$t_s = (a_B/c_s).$$

The shock dynamics of the warm dense electron gas using a quantum hydrodynamic model

F. Graziani, **Z. Moldabekov**, B. Olson, M. Bonitz, Contrib. Plasma Phys. 2022;62:e202100170.

Shock propagation in a quantum electron gas

Conclusions:

1. From the numerical hydrodynamic simulations we observe that the quantum Bohm pressure induces shear force which weakens the formation and strength of the shock.

2. Our theoretical and numerical analysis allows us to identify characteristic dimensionless shock propagation parameters at which the effect of the Bohm force is important.

For more details see:

[1] **Z. A. Moldabekov**, T. Dornheim, G. Gregori, F. Graziani, M. Bonitz, A. Cangi, "*Towards a Quantum Fluid Theory of Correlated Many-Fermion Systems from First Principles*," **SciPost Physics *12***, *062 (2022)*

[2] F. Graziani, **Z. Moldabekov**, B. Olson, M. Bonitz, *Shock Physics in Warm Dense Matter--a quantum hydrodynamics perspective*, Contrib. Plasma Phys. 2022;62:e202100170

For interested students, please see our recent relevant publications

CASUS
CENTER FOR ADVANCED SYSTEMS UNDERSTANDING

[1] **Z. Moldabekov**, J. Vorberger, T. Dornheim, **J. Chem. Theory Comput.** 18, 5, 2900–2912 (2022)

[2] **Z. Moldabekov**, A. Cangi, J. Vorberger, and T. Dornheim, **Phys. Rev. B** 105, 035134 (2022)

[3] **Z. Moldabekov**, T. Dornheim, M. Boehme, J. Vorberger, and A. Cangi, **J. Chem. Phys.** 155, 124116 (2021).

[4] **Z. Moldabekov**, T. Dornheim, G. Gregori, F. Graziani, M. Bonitz, A. Cangi, **SciPost Phys.** 12, 062 (2022).

[5] **Z. Moldabekov**, T. Dornheim, & A. Cangi, **Sci Rep** 12, 1093 (2022).

[6] **Z. Moldabekov**, M. Böhme, J. Vorberger, D. Blaschke, T. Dornheim, **arXiv:2209.00928** (2022)

[7] **Z. Moldabekov**, M. Lokamani, J. Vorberger, A.Cangi, T. Dornheim, **arXiv:2212.00644** (2022)

[8] M.Böhme, **Z. Moldabekov**, J. Vorberger, and T. Dornheim, **Phys. Rev. Lett.** 129, 066402 (2022)

[9] F. Graziani, **Z. Moldabekov**, B. Olson, M. Bonitz, **Contrib. Plasma Phys.** 2022;62:e202100170 (2022)

Acknowledgment

HZDR

Dr. T. Dornheim | M. Böhme

Dr. A. Cangi | Dr. J. Vorberger

Uni Kiel

Prof. M. Bonitz

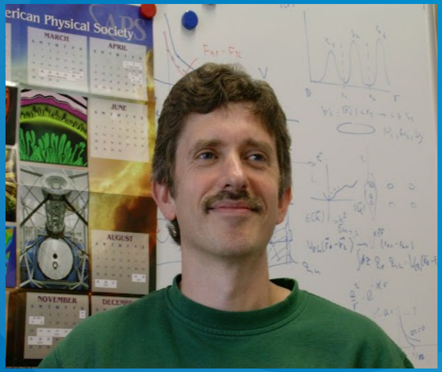

Uni. Wrocławski

Prof. D. Blaschke

Uni. Oxford

Prof. G. Gregori

LLNL

Dr. F. Graziani

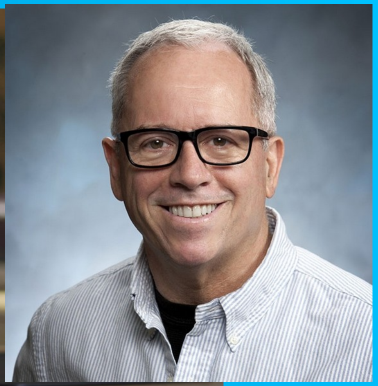

CASUS

CENTER FOR ADVANCED SYSTEMS UNDERSTANDING

www.casus.science